

Exciton-polaritons in transition-metal dichalcogenides and their direct excitation via energy transfer

Yuri N. Gartstein,^{1,*} Xiao Li,^{2,1} and Chuanwei Zhang^{1,†}

¹*Department of Physics, The University of Texas at Dallas, Richardson, Texas, 75080, USA*

²*Department of Physics, The University of Texas at Austin, Austin, Texas 78712, USA*

Excitons, composite electron-hole quasiparticles, are known to play an important role in optoelectronic phenomena in many semiconducting materials. Recent experiments and theory indicate that the band-gap optics of the newly discovered monolayer transition-metal dichalcogenides (TMDs) is dominated by tightly bound valley excitons. The strong interaction of excitons with long-range electromagnetic fields in these 2D systems can significantly affect their intrinsic properties. Here, we develop a semi-classical framework for intrinsic exciton-polaritons in monolayer TMDs that treats their dispersion and radiative decay on the same footing and can incorporate effects of the dielectric environment. It is demonstrated how both inter- and intra-valley long-range interactions influence the dispersion and decay of the polaritonic eigenstates. We also show that exciton-polaritons can be efficiently excited via resonance energy transfer from quantum emitters such as quantum dots, which may be useful for various applications.

PACS numbers: 78.20.-e, 73.22.Pr

Introduction. Monolayer molybdenum disulfide MoS₂ and other group-VI transition-metal dichalcogenides (TMDs) are novel two-dimensional (2D) semiconductor systems whose electronic and optical properties attract a great deal of attention [1–27]. One of their prominently discussed features is the opportunity to manipulate the valley degree of freedom, including by optical means due to opposite-handed circular polarizations of the inter-band transitions in the two valleys [4]. A growing experimental and theoretical evidence [2–8, 17–27] indicates that the band-gap optical properties of monolayer TMDs are dominated by relatively tightly bound electron-hole pairs, excitons, with binding energies substantially larger than in the majority of conventional inorganic semiconductor quantum wells [28, 29]. The corresponding 2D exciton physics in TMDs may therefore reflect generally stronger interactions of excitons with macroscopic electric fields and light.

An important fundamental issue is the nature of intrinsic excitonic eigenstates and their energy-momentum (dispersion) relationships. It was shown recently [22] that the long-range exchange Coulomb interaction mixes individual valley excitons to establish excitons with the longitudinal (L) and transverse (T) polarizations as normal system modes, similarly to quantum well excitons [30, 31]. The resulting exciton spectrum, as a function of its center-of-mass in-plane wave-vector $\mathbf{k} = (k_x, k_y) = k(\cos\theta, \sin\theta)$, was found to exhibit a specific Dirac-cone-like behavior at low momenta $\hbar k$, in particular within the light cone, $k < q = \omega/c$. As we perform in this Letter a semi-classical analysis of the interaction of monolayer excitons with long-range electromagnetic fields, it will be shown however that (1) the dispersion of L - and T -excitons is affected via *both* inter- and intra-valley processes leading to the overall generic behavior characteristic of the 2D excitons [30–33] without a Dirac-cone fea-

ture; (2) Moreover, also in a general fashion, the intrinsic behavior within and in the vicinity of the light cone is that of the 2D exciton-polaritons as determined by the full electromagnetic (rather than just electrostatic) mixing of valley excitons taking account of the retardation effects [29, 33]. (In the electrostatic limit the obtained dispersion reproduces the exciton spectrum that we derive from inter- and intra-valley exchange Coulomb interactions). General features of the intrinsic exciton-polaritons are clearly accentuated in the macroscopic electrodynamics framework, which allows for a straightforward generalization of the analysis of the polariton dispersion and radiative decay in free-standing monolayer TMDs to monolayers at the interface between different media. We also use that framework to illustrate the possibility of very efficient direct excitation of monolayer polaritons by energy transfer from proximal electric-dipole emitters such as quantum dots, which may be useful for various applications.

Exciton-polaritons from effective dipole-dipole interactions. In a common basic description of optically active lowest energy excitons in monolayer TMDs, they arise as a result of the direct Coulomb attraction between an electron and a hole in the same valley. Due to the strong spin-orbit coupling in TMDs, the electron-hole spin composition is associated with the valley [4] and therefore will be omitted. In the valley-based picture there are then two exciton species (index $\alpha = 1, 2$) corresponding to two different valleys, both having the same energy dispersion

$$E_0(\mathbf{k}) = \hbar\omega_0(k) = \hbar\omega_0 + \hbar^2 k^2 / 2M_0, \quad (1)$$

where $\hbar\omega_0$ is typically somewhat below 2 eV and the exciton mass M_0 is close to the free electron's m_e [8, 10, 19, 22]. The parabolic kinetic energy in Eq. (1) with M_0 being the sum of electron and hole effective

masses signifies the fact that the exciton propagation in space is enabled by the simultaneous motion of the electron and hole. The inclusion of the standard exchange Coulomb interaction results in another mechanism of the exciton propagation and concomitant modifications of its dispersion, which can be seen as the electric field of the exciton annihilated at one spatial point creating the exciton at another point. Such a long-range process is well-known to correspond to the electrostatic dipole-dipole coupling, which is the major exciton transfer mechanism in molecular systems [33]. This physically attractive semiclassical real-space picture can then be readily extended to the dipole-dipole coupling mediated by the full electromagnetic interactions with the retardation effects in place. The resulting intrinsic excitations, exciton-polaritons, would thus take into account the exciton-light interaction absent in the picture of Coulomb excitons derived with electrostatic interactions alone [29, 32, 33].

The electromagnetic interactions in monolayer TMDs may be classified as intra-valley ($\alpha = \beta$) and inter-valley ($\alpha \neq \beta$) couplings, in some analogy with bipartite lattices and molecular systems with two molecules per unit cell [33]. Correspondingly, the exciton self-energy correction due to the interactions is a 2×2 matrix Σ . In the continuum description of 2D Wannier-Mott excitons, it can be written in the form of

$$\Sigma_{\alpha\beta}(E, \mathbf{k}) = \int d\mathbf{r} v_{\alpha\beta}(\mathbf{r}) e^{i\mathbf{k}\cdot\mathbf{r}}, \quad (2)$$

as a function of energy $E = \hbar\omega = \hbar cq$ and wave-vector \mathbf{k} variables. Here $v_{\alpha\beta}(\mathbf{r}) = |\psi(0)|^2 V_{\alpha\beta}(\mathbf{r})$ is the 2D energy density determined by the probability $|\psi(0)|^2 = 8/(\pi a_B^2)$ of finding the electron and hole of the exciton at the same spatial point [29] and the interaction matrix elements $V_{\alpha\beta}(\mathbf{r})$ dependent on the relative two-dimensional position $\mathbf{r} = r\hat{\mathbf{r}}$. From *Ab initio* calculations [8, 11, 21, 24], the exciton Bohr radius in monolayer TMDs is estimated as $a_B \sim 1$ nm. For the free-standing monolayers in vacuum the long-range part of the interaction

$$V_{\alpha\beta}(\mathbf{r}) = \frac{e^{iqr}}{r} \left\{ q^2 \left[(\hat{\mathbf{r}} \cdot \mathbf{d}_\alpha^{f0})(\hat{\mathbf{r}} \cdot \mathbf{d}_\beta^{of}) - \mathbf{d}_\alpha^{f0} \cdot \mathbf{d}_\beta^{of} \right] + \left(\frac{1}{r^2} - \frac{iq}{r} \right) \left[\mathbf{d}_\alpha^{f0} \cdot \mathbf{d}_\beta^{of} - 3(\hat{\mathbf{r}} \cdot \mathbf{d}_\alpha^{f0})(\hat{\mathbf{r}} \cdot \mathbf{d}_\beta^{of}) \right] \right\} (3)$$

as arising from the full electromagnetic dipole-dipole coupling (in Gaussian units) [34]. The familiar electrostatic limit corresponds to the light vacuum wave number $q = \omega/c \rightarrow 0$ (speed of light $c \rightarrow \infty$). The interacting α and β species in Eq. (3) are represented by the corresponding interband dipole transition matrix elements for creation, \mathbf{d}_α^{f0} , and annihilation, \mathbf{d}_β^{of} , of electron-hole pairs. In the electrostatic limit, the self-energy corrections (2) would be real-valued and functions of wave vector \mathbf{k} only. With the retarded electric fields, however, $\Sigma_{\alpha\beta}$ are functions of both energy and wave-vector vari-

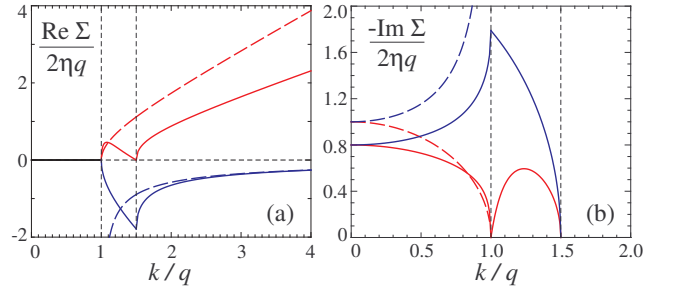


FIG. 1: Functional behavior of the (a) real and (b) imaginary parts of the intrinsic exciton-polariton self-energy as per Eqs. (6) and (10). Red color lines are used for the longitudinal (L) and blue for the transverse (T) excitons. Shown with dashed lines are the results for a free-standing monolayer in vacuum, and solid lines are for the monolayer on a glass-like substrate, see text.

ables and generally complex-valued; they would therefore determine both the exciton dispersion and the decay width (decay into photons) in a self-consistent calculation. Calculations with the retarded fields are equivalent [35] to calculations of exciton-polaritons as arising from the interaction of Coulomb excitons with transverse photons [29, 33].

The in-plane interband dipole transition matrix elements $\mathbf{d}_\alpha^{(\alpha)} = (d_x^{(\alpha)}, id_y^{(\alpha)})$ have a common form for both valleys but with the opposite handedness of their circular polarization:

$$d_x^{(1)} = d_y^{(1)} = d_x^{(2)} = -d_y^{(2)} = \mathcal{D}, \quad (4)$$

where we chose \mathcal{D} as a real positive quantity. From a two-band monolayer TMD model [4], for instance, the dipole transition moment would be $\mathcal{D} = eat/E_g$, where e is the fundamental charge, a the lattice structure constant ($\simeq 3.19$ Å), t the nearest neighbor hopping integral ($\simeq 1.10$ eV) and E_g the energy gap between the conduction and valence bands that the excitons come from. A calculation based on the three-band model [23] gives the same form, but with a slightly different value of t .

The difference between the transition dipole moments (4) in the two valleys translates into the difference of inter- and intra-valley couplings (3). A direct calculation of integrals in Eq. (2) then leads to the following \mathbf{k} -dependence of the self-energy matrix [36]:

$$\Sigma(E, \mathbf{k}) = \begin{pmatrix} J_0 & \exp(-2i\theta) J_1 \\ \exp(2i\theta) J_1 & J_0 \end{pmatrix}, \quad (5)$$

where the intra-valley component $J_0 = -i\eta(\sqrt{q^2 - k^2} + q^2/\sqrt{q^2 - k^2})$ and the inter-valley component $J_1 = i\eta k^2/\sqrt{q^2 - k^2}$ feature the same magnitude scale $\eta = 2\pi|\psi(0)|^2 \mathcal{D}^2$. The functional form of these components illustrates the great qualitative distinction resulting from the retarded interactions: the obtained corrections J_0

and J_1 are purely imaginary above the light line, $k < q$, but become purely real ($\sqrt{q^2 - k^2} \rightarrow i\sqrt{k^2 - q^2}$) below the light line, $k > q$. As is known [32, 33], this signifies the impossibility for the intrinsic 2D exciton-polariton with $k > q$ to decay into a photon due to the momentum conservation. Exciton-polaritons with $k < q$, on the other hand, exhibit the radiative width due to such a decay. Moreover this width is greatly enhanced in comparison with localized emitters [33]. It is also instructive to look at the electrostatic limit ($q \rightarrow 0$) of these corrections: the inter-valley component then becomes $J_1 = \eta k$, precisely the result derived in Ref. [22]. Importantly, the intra-valley component J_0 becomes equal to J_1 in this limit, which is also confirmed in our independent calculations with the exchange Coulomb interaction.

Because of the inter-valley coupling J_1 , the valley excitations are clearly not the eigenstates of the system. Instead, the eigenstates are their linear combinations $\Psi_{\pm} = 2^{-1/2} \begin{pmatrix} 1 \\ \pm \exp(2i\theta) \end{pmatrix}$ that diagonalize matrix Σ and yield the corresponding self-energy corrections as

$$\Sigma_{\pm} = J_0 \pm J_1 = -2i\eta \times \begin{cases} \sqrt{q^2 - k^2}, & (L), \\ q^2/\sqrt{q^2 - k^2}, & (T). \end{cases} \quad (6)$$

These eigenstates have, respectively, longitudinal, for Ψ_+ , and transverse, for Ψ_- , polarizations with respect to polariton wave-vector \mathbf{k} [22]: for the propagation along the x -axis, e.g., Eq. (4) shows that Ψ_+ combination corresponds to the transition moment $\propto (\mathcal{D}, +i\mathcal{D}) + (\mathcal{D}, -i\mathcal{D})$ along x while Ψ_- to the moment $\propto (\mathcal{D}, +i\mathcal{D}) - (\mathcal{D}, -i\mathcal{D})$ along y . The functional forms of self-energy corrections (6) for the free-standing monolayer are shown in Fig. 1 by dashed lines. It is clear that, in the electrostatic limit, only the L -excitons would acquire the additional term $\Sigma_+ = 2\eta k$ in their dispersion due to long-range exchange interactions, while the dispersion of T -excitons would remain unchanged ($\Sigma_- = 0$) as Eq. (1). There is no Dirac-cone-like behavior even in the electrostatic limit. In the valley-centric basis these conclusions thus follow from the simultaneous account of both inter- and intra-valley processes as opposed to the inter-valley coupling alone [22].

Exciton-polaritons from macroscopic Maxwell equations. The obtained results for polaritonic eigenstates are in agreement with the picture known for quantum wells [30] and reflect the fact that the opposite-handedness in-plane susceptibilities χ_1 and χ_2 of the individual valleys just add up in the overall *isotropic* electrodynamic response of the monolayer. The latter is then characterized by the scalar susceptibility χ defining the monolayer 2D current density $\mathbf{j} = -4\pi i\omega\chi\mathbf{E}$ induced by the in-plane electric field \mathbf{E} . It is this current density that enters the boundary conditions for the macroscopic Maxwell equations determining the effects of long-range fields on the system excitations [29, 33]. For well-separated excitonic states (1), e.g., the 2D scalar susceptibility acquires a

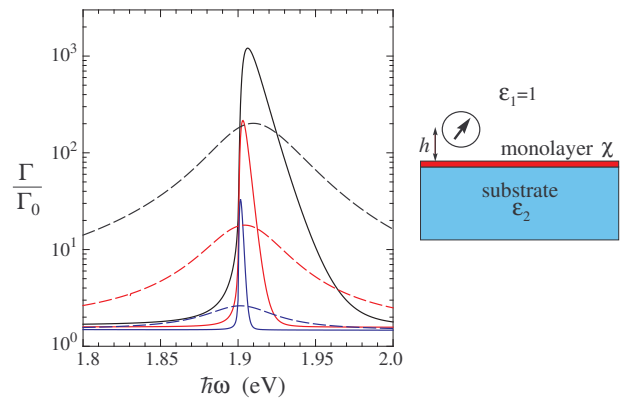


FIG. 2: Acceleration of the decay rate Γ of a randomly oriented electric dipole emitter such as quantum dots in the vicinity of the monolayer on a glass-like substrate as compared to the spontaneous decay rate Γ_0 in vacuum, Eq. (11). The data are shown as a function of the emitter frequency ω and for different distances h to the interface: 5 nm (black lines), 10 nm (red) and 20 nm (blue). Solid lines display results for the nearly dissipationless excitons ($\gamma = 0.1$ meV), dashed lines are for the dissipation parameter $\gamma = 25$ meV. These illustrative calculations were done with the model parameters $4\pi\chi_0 = 2$ nm, $4\pi\hbar^2 A = 0.25$ eV²·nm in Eq. (7) and $\hbar\omega_0 = 1.9$ eV, $M_0 = m_e$ in Eq. (1).

familiar single-oscillator form

$$\chi(\omega, k) = \chi_0 + A/(\omega_0^2(k) - \omega^2 - 2i\gamma\omega), \quad (7)$$

where χ_0 is the background term due to higher-frequency transitions and γ the phenomenological dissipation parameter. A many-oscillator form could be used to include even more specifics for different TMD monolayers.

The versatile macroscopic framework can be easily applied to various environments. Here we exemplify this by considering the model of an infinitesimally thin planar monolayer between two non-magnetic media with dielectric constants ε_1 and ε_2 . One can solve for the eigenfrequencies of the system directly. Alternatively, as also useful for other problems, one looks at the poles of the reflection coefficients for electromagnetic waves in our sandwich configuration. The 3D setup involves not only the in-plane components of the fields and wave vectors but also their z -components perpendicular to the planar interface. With the boundary conditions of the polarizable interface monolayer [37], one easily derives the reflection coefficient amplitudes for p - and s -polarized waves as (ω, k) -dependent

$$r^{(p)} = \left(\frac{\varepsilon_2}{k_{z2}} - \frac{\varepsilon_1}{k_{z1}} - 4\pi i\chi \right) \left(\frac{\varepsilon_2}{k_{z2}} + \frac{\varepsilon_1}{k_{z1}} - 4\pi i\chi \right)^{-1} \quad (8)$$

and

$$r^{(s)} = (k_{z1} - k_{z2} + 4\pi i q^2 \chi) (k_{z1} + k_{z2} - 4\pi i q^2 \chi)^{-1}. \quad (9)$$

The normal components $k_{zi} = (\varepsilon_i q^2 - k^2)^{1/2}$ of the waves in the respective media appear, as usual [38], related to the in-plane wave number k for given frequency $\omega = cq$. The in-plane component of the electric field in a p -polarized wave is along the in-plane wave vector \mathbf{k} whereas in an s -polarized wave they are perpendicular to each other. Hence, the poles of Eq. (8) determine the dispersion and decay of the L -polaritons while poles of Eq. (9) those of the T -polaritons. Writing the pole equations in the form of

$$-\frac{1}{\chi} = -4\pi i \times \begin{cases} (\varepsilon_1/k_{z1} + \varepsilon_2/k_{z2})^{-1}, & (L), \\ q^2/(k_{z1} + k_{z2}), & (T), \end{cases} \quad (10)$$

one recognizes that the functional dependence in the r. h. s. of Eq. (10) reduces to that in Eq. (6) for the free-standing monolayer. It is also clear that with the negligible dissipation and screening due to higher-frequency transitions, $-1/\chi \simeq 2\omega_0(\omega - \omega_0(k))/A$ becomes just proportional to the self-energy corrections in the vicinity of the resonance, $\omega \simeq \omega_0$. The derivation with the effective dipole-dipole interactions thus fully agrees with the macroscopic electrodynamics result, and we obtain $A = 2\omega_0\eta/\pi\hbar$ by comparing Eqs. (6) and (10). Note that the screening by the surrounding can substantially affect the exciton radius and binding energy reducing thus “the strength” A of the resonance (7); the calculations of exciton binding are outside of our scope.

Figure 1 illustrates the differences in the behavior of self-energy corrections for two systems: the symmetric sandwich with $\varepsilon_1 = \varepsilon_2 = 1$ (a free standing monolayer) and the asymmetric sandwich with $\varepsilon_1 = 1$ and $\varepsilon_2 = 2.25$ (glass-like substrate), as follows from Eq. (10). It is transparent that in the symmetric case, the T -polariton branch exhibits splitting at the light cone, $k \rightarrow q$, as consistent with the divergence of the radiative decay rate (6) at $k \rightarrow q = 0$. Qualitatively differently for the asymmetric sandwich, there is no divergence in the decay rate and the dispersion of the T -polariton branch is continuous. Figure 1(b) also shows the extension of the region of the radiative decay: polaritons with $q < k < \sqrt{\varepsilon_2}q$ can now decay into photons that propagate only in the substrate. Beyond that region, however, the intrinsic (without scattering effects) polaritons become non-radiative and, conversely, cannot be directly excited by plane-wave photons incident on the monolayer from the infinity, the situation similar to the excitation of surface waves like surface plasmons [32, 33, 38].

Application to energy transfer. The direct excitation of non-radiative modes is however known to be possible by the near electromagnetic fields. This may be accomplished, e.g., with special optical geometry setups [32, 33, 38] or via resonance energy transfer (ET) from proximal quantum emitters such as molecules or quantum dots [38–40]. We note that ET from 0D emitters to (quasi) 2D absorbers has been of increasing theoretical and experimental interest, including organic and inor-

ganic semiconductors [41], graphene [42] and MoS₂ [43] (and references therein). ET provides a new decay channel and is thus manifested in the acceleration of the observed emitter’s photoluminescence decay.

Using the macroscopic electrodynamics formalism developed for such applications [38, 40], the decay rate Γ of the randomly-oriented electric-dipole emitter in the medium with dielectric constant ε_1 at distance h from the planar interface is derived [38] as

$$\Gamma/\Gamma_1 = 1 + (1/2k_1^3) \operatorname{Re} \int_0^\infty (k dk/k_{z1}) e^{2ik_{z1}h} \times \left((2k^2 - k_1^2)r^{(p)} + k_1^2 r^{(s)} \right), \quad (11)$$

where Γ_1 is the spontaneous decay rate in the uniform medium and $k_1^2 = \varepsilon_1 q^2$. The integration in Eq. (11) over all values of the in-plane wave-vectors k signifies that the near-fields of the emitter are included. Figure 2 illustrates the results following from Eq. (11) with the reflection coefficients (8) and (9) for the considered geometry. The analysis shows that a very large effect observed in Figure 2 is predominantly due to the excitation of L -polaritons (poles of $r^{(p)}$), similar to a very efficient excitation of surface plasmons by ET [39, 40]; the dispersion of the peak with distance h is also clearly seen. For the computational illustration here we used a more moderate value of the resonance strength A in Eq. (7), and its larger values would lead to even faster ET into the monolayer. Figure 2 also shows how the narrower polariton peaks are spread by exciton damping (γ) processes. Excitation of TMD monolayer polaritons via high efficiency ET from neighboring emitters might be attractive for various optoelectronic applications [43, 44]. Its experimental studies for different emitter frequencies and distances could be used for quantification of polariton properties.

Discussion. While our discussion in this paper has been focussed on the intrinsic polaritons, it is recognized that various scattering processes due to polariton interactions with phonons and defects can significantly affect the observable optical properties of realistic TMDs, and this appears as an important topic for future studies. Just as with the quantum well polaritons, e.g., their thermalization may lead to a specific temperature dependence of the radiative lifetime. With the substantial contribution to polariton dispersion in TMDs from the long-range interactions we discussed, that temperature dependence may deviate from the dependence resulting from the purely parabolic exciton dispersion [45].

Finally, we estimate the experimentally relevant parameters for MoS₂. Following Ref. [22], η would be estimated as ~ 0.75 eV·Å, resulting in substantial contributions to the exciton dispersion. With this estimate, the energy unit in Fig. 1 $2\eta q \sim 1.5$ meV for $q = \omega/c \sim 0.01$ nm⁻¹. Likewise, one would obtain $4\pi\hbar^2 A \sim 1.1$ eV²·nm for the unscreened value of the parameter A in Eq. (7).

Acknowledgements: YNG is grateful to NSF for the support provided through the DMR-1207123 grant. XL and CZ are supported by ARO (W911NF-12-1-0334) and AFOSR (FA9550-13-1-0045).

* Electronic address: yuri.gartstein@utdallas.edu

† Electronic address: chuanwei.zhang@utdallas.edu

- [1] A. K. Geim and I. V. Grigorieva, *Van der Waals heterostructures*, Nature **499**, 419 (2013).
- [2] X. Xu, W. Yao, D. Xiao, and T. F. Heinz, *Spin and pseudospins in layered transition metal dichalcogenides*, Nature Physics **10**, 343 (2014).
- [3] K. F. Mak, C. Lee, J. Hone, J. Shan, and T. F. Heinz, *Atomically thin MoS₂: A new direct-gap semiconductor*, Phys. Rev. Lett. **105**, 136805 (2010).
- [4] D. Xiao, G.-B. Liu, W. Feng, X. Xu, and W. Yao, *Coupled Spin and Valley Physics in Monolayers of MoS₂ and Other Group-VI Dichalcogenides*, Phys. Rev. Lett. **108**, 196802 (2012).
- [5] H. Zeng, J. Dai, W. Yao, D. Xiao, and X. Cui, *Valley polarization in MoS₂ monolayers by optical pumping*, Nat. Nanotech. **7**, 490 (2012).
- [6] K. F. Mak, K. He, J. Shan, and T. F. Heinz, *Control of valley polarization in monolayer MoS₂ by optical helicity*, Nat. Nanotech. **7**, 494 (2012).
- [7] T. Cao *et al.*, *Valley-selective circular dichroism of monolayer molybdenum disulfide*, Nat. Comm. **3**, 887 (2012).
- [8] J. S. Ross, *et al.* *Electrical control of neutral and charged excitons in a monolayer semiconductor*, Nature Comm. **4**, 1474 (2013).
- [9] Y. Zhang, *et al.* *Direct observation of the transition from indirect to direct bandgap in atomically thin epitaxial MoSe₂*, Nat. Nanotech **9**, 111 (2014).
- [10] K. F. Mak, *et al.* *Tightly bound trions in monolayer MoS₂*, Nature Mater. **12**, 207 (2013).
- [11] J. Feng, X. Qian, C.-W. Huang, and J. Li, *Strain-engineered artificial atom as a broad-spectrum solar energy funnel*, Nature Photonics **6**, 866 (2012).
- [12] D. Lagarde, *et al.* *Carrier and polarization dynamics in monolayer MoS₂*, Phys. Rev. Lett. **112**, 047401 (2014).
- [13] K. F. Mak, K. L. McGill, J. Park, P. L. McEuen, *The Valley Hall Effect in MoS₂ Transistors*, Science **344**, 1489 (2014).
- [14] B. W. H. Baugher, H. O. H. Churchill, Y. Yang, and P. Jarillo-Herrero, *Intrinsic electronic transport properties of high-quality monolayer and bilayer MoS₂*. Nano Lett. **13**, 4212 (2013).
- [15] X. Li, F. Zhang, Q. Niu, *Unconventional Quantum Hall Effect and Tunable Spin Hall Effect in Dirac Materials: Application to an Isolated MoS₂ Trilayer*, Phys. Rev. Lett. **110**, 066803 (2013).
- [16] R.-L. Chu, X. Li, S. Wu, Q. Niu, W. Yao, X. Xu, C. Zhang, *Valley-splitting and valley-dependent inter-Landau-level optical transitions in monolayer MoS₂ quantum Hall systems*, Phys. Rev. B **90**, 045427 (2014).
- [17] A. M. Jones, *et al.* *Spin-layer locking effects in optical orientation of exciton spin in bilayer WSe₂*. Nature Phys. **10**, 130 (2014).
- [18] G. Aivazian, *et al.*, *Magnetic Control of Valley Pseudospin in Monolayer WSe₂*, arXiv:1407.2645 (2014).
- [19] A. M. Jones *et al.*, *Optical generation of excitonic valley coherence in monolayer WSe₂*, Nat. Nanotech. **8**, 634 (2013).
- [20] S. Wu, *et al.*, *Electrical tuning of valley magnetic moment through symmetry control in bilayer MoS₂*, Nat. Phys. **9**, 149 (2013).
- [21] D. Y. Qiu, F. H. da Jornada, and S. G. Louie, *Optical Spectrum of MoS₂: Many-Body Effects and Diversity of Exciton State*, Phys. Rev. Lett. **111**, 216805 (2013).
- [22] H. Yu, G. Liu, P. Gong, X. Xu, W. Yao, *Bright excitons in monolayer transition metal dichalcogenides: from Dirac cones to Dirac saddle points*, Nat. Commun. **5**, 3876 (2014).
- [23] G.-B. Liu, W.-Y. Shan, Y. Yao, W. Yao, D. Xiao, *Three-band tight-binding model for monolayers of group-VIB transition metal dichalcogenides*, Phys. Rev. B **88**, 085433 (2013).
- [24] T. C. Berkelbach, M. S. Hybertsen, and D. R. Reichman, *Theory of neutral and charged excitons in monolayer transition metal dichalcogenides*, Phys. Rev. B **88**, 045318 (2013).
- [25] G. Berghauser and E. Malic, *Analytical approach to excitonic properties of MoS₂*, Phys. Rev. B **89**, 125309 (2014).
- [26] A. Ramasubramaniam, *Large excitonic effects in monolayers of molybdenum and tungsten dichalcogenides*, Phys. Rev. B **86**, 115409 (2012).
- [27] F. Wu, F. Qu, A. H. MacDonald, *Exciton band structure of monolayer MoS₂*, arXiv:1501.02273 (2015).
- [28] P. K. Basu, *Theory of optical processes in semiconductors, Bulk and microstructures*, (Oxford: Clarendon Press, 1997).
- [29] H. Haug and S. W. Koch, *Quantum theory of the optical and electronic properties of semiconductors* (Singapore: World Scientific, 2004).
- [30] L. Andreani and F. Bassani, *Exchange interaction and polariton effects in quantum-well excitons*, Phys. Rev. B **41**, 7536 (1990).
- [31] R. Girlanda, S. Savasta, and B. Azzarboni, Riv. Nuovo Cim. **21**, 1 (1998).
- [32] V. M. Agranovich and V. L. Ginzburg, *Crystal Optics with Spatial Dispersion, and Excitons* (Springer, Berlin, 1984).
- [33] V. M. Agranovich, *Excitations in Organic Solids* (Oxford University Press, Oxford, 2009).
- [34] J. D. Jackson, *Classical Electrodynamics* (Wiley, New York, 1975).
- [35] Y. N. Gartstein, and V. M. Agranovich, *Excitons in long molecular chains near the reflecting interface*, Phys. Rev. B **76**, 115329 (2007).
- [36] The integral (2) with interaction (3) would formally diverge due to the short-distance $\propto 1/r^3$ behavior of the electrostatic dipole-dipole coupling. Of course, at short distances the point-dipole description does not apply, whereas the actual short-range Coulomb interactions would be determined by the detailed behavior of electron wave functions. The divergent electrostatic term needs therefore to be separated in the calculation. The separated term represents a constant overall renormalization shift Σ_0 of the exciton energies due to short-range interactions that we are not interested in.
- [37] We restrict our attention here to the layer with the in-plane polarizability only. With account of the polarizability perpendicular to the layer, the expression for the

- reflection coefficient $r^{(p)}$ is more involved than Eq. (8).
- [38] L. Novotny and B. Hecht, *Principles of Nano-Optics*, (Cambridge University Press, Cambridge, 2006).
- [39] M. R. Philpott, *J. Chem. Phys.* **62**, 1812 (1975).
- [40] R. R. Chance, A. Prock, and R. Silbey, in *Advances in Chemical Physics*. Vol. 37, edited by S. A. Rice and I. Prigogine (Wiley, New York, 1978) pp. 1–65.
- [41] J. M. Gordon and Y. N. Gartstein, *Dielectric polarization, anisotropy and nonradiative energy transfer into nanometre-scale thin semiconducting films*, *J. Phys.: Condens. Matter* **25**, 425302 (2013).
- [42] L. Gaudreau, K. J. Tielrooij, G. E. D. K. Prawiroatmodjo, J. Osmond, F. J. G. de Abajo, and F. H. L. Koppen, *Universal Distance-Scaling of Nonradiative Energy Transfer to Graphene*, *Nano Lett.* **13**, 2030 (2013).
- [43] F. Prins, A. J. Goodman, and W. A. Tisdale, *Reduced Dielectric Screening and Enhanced Energy Transfer in Single- and Few-Layer MoS₂*, *Nano Lett.* **14**, 6087 (2014).
- [44] V. M. Agranovich, Y. N. Gartstein, and M. Litinskaya, *Hybrid Resonant Organic-Inorganic Nanostructures for Optoelectronic Applications*, *Chem. Rev.* **111**, 5179 (2011).
- [45] J. Feldman, G. Peter, E. O. Göbel, P. Dawson, K. Moore, C. Foxon, and R. J. Elliott, *Linewidth dependence of radiative exciton lifetimes in quantum wells*, *Phys. Rev. Lett.* **59**, 2337 (1987).